Electron microscopy of nuclear graphite: A modelling approach

C.R. Seabourne[1], R. Brydson[1], M.I. Heggie[2], C.D. Latham[2] and A.J. Scott[1]
[1]Institute for Materials Research, SPEME, University of Leeds, Leeds, LS2 9JT, United Kingdom
[2]Chemistry Subject Group, School of Life Sciences, University of Sussex, Falmer, Brighton, East Sussex, BN1 9QJ, United Kingdom
c.r.seabourne@leeds.ac.uk

Abstract. Graphite acts as both a major structural component and moderator in nuclear reactors. Upon neutron irradiation, various structural and property changes occur. Property changes include; coefficient of thermal expansion (CTE), Young's modulus and thermal resistivity. This work focuses on the characterisation of irradiated graphite models using both electron energy-loss spectroscopy (EELS) and imaging techniques. A number of models of irradiated graphite have been found, whereby one or more interstitial atoms form between the hexagonal layers. In this work, density functional theory (DFT) modelling is used to predict EEL spectra (carbon K edges) at the spiro-interstitial position, and contrast those to bulk predictions. We observe that for a 'bulk-like' position in the spiro-interstitial model, the carbon K edge shape is similar to that of true bulk, thus confirming the validity of the model used. For the carbon K edge prediction at the spiro-interstitial position, although peaks in the π* region remain in approximately the same energy positions, there is considerable broadening suggesting the presence of strained sp^2 bonding character. The σ* peak is significantly altered, both in energy position and intensity relative to the π* region. These observations are arguably consistent with a spiro-interstitial strained from the ideal bonding angles observed in spiro-pentane. Simulations of TEM and HAADF images of the spiro-interstitial model were also performed. These suggested that in a typical TEM, for the (100) orientation, even at a thickness of ~15 Å the interstitial would be difficult to observe. In the case of (S)TEM, a similar situation exists.

1. Introduction

Graphite is a major structural component as well as a moderator in nuclear reactors. It is likely to continue to be used in high temperature reactors (HTRs), which are currently being planned. These are projected to have an operating lifetime of between 50 and 100 years [1]. Over the course of a reactor's lifetime, neutron irradiation of graphite causes various structural and property changes, including for example Young's modulus and the thermal resistivity [2–3]. A new EPSRC consortium, 'Fundamentals of Nuclear Graphite' has been established, involving the authors of this work. Nanoscale characterisation techniques have been markedly improved since the original theories regarding irradiation damage were developed. A major aim therefore of the consortium is to improve the mechanistic understanding of the damage processes.

On the atomic level, a number of models of irradiated graphite have been developed, and the overwhelming majority invoke Frenkel pairs as the principal defects arising [4]. Here we examine a single interstitial (di-interstitials are also possible) to see if it could be observable in the electron microscope. The ground state for a single interstitial is the 'spiro-interstitial' structure, so-called due to its resemblance to spiro-pentane [5–7].

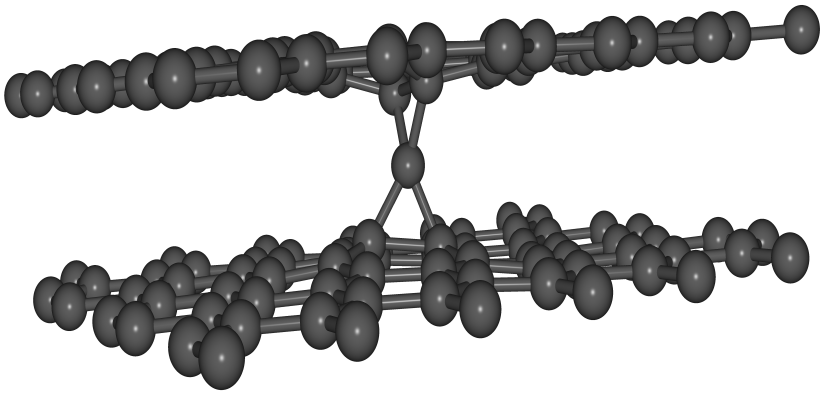

Figure 1. The 'spiro-interstitial' structure of irradiated graphite. This is the ground state structure for a single interstitial, the formation energy relative to pure graphite is 5.85 eV [6].

The CASTEP density functional theory (DFT) code is used to predict EEL spectra [8]. Image simulation in the electron microscope is also investigated, using a multislice methodology for TEM simulations, and the QSTEM code for (S)TEM imaging [9–11].

2. Methodology

In terms of EELS simulations, the employed methodology was similar to previous work involving some of the authors of this paper [12-13]. Throughout the DFT calculations presented, the local density approximation (LDA) was used, consistent with previous work in this field, which was used to form the basis of the structural models in this paper [6]. In terms of other parameters, there are two major considerations; the basis set size (defined by the kinetic energy cut-off value) and the density of *k*-point sampling. These values were converged specifically against the predicted carbon K edge. The kinetic energy cut-off value was increased in steps of 100 eV from 200 eV. The *k*-point mesh density was doubled from $4\times4\times4$ upwards. A Monkhorst-Pack grid of *k*-points was used, with equal numbers of points along each reciprocal lattice direction, thus increasing the sampling density in the *c* direction. The successive predicted K edge spectra (ground state predictions) were analysed numerically. For example, upon doubling the *k*-point mesh density, the percentage change in intensity value was found for each energy-axis value, these then being averaged across a range of −5 eV to 50 eV above the Fermi level. Convergence was achieved when this average percentage was less than 15%. Practically speaking, once broadening is applied much less rigorous parameters would lead to highly similar results.

Table 1. Chosen parameters for bulk graphite carbon K edge modelling.

Parameter	Value
Kinetic energy cut-off	500 eV
EELS calculation *k*-point mesh	32×32×32

High-resolution TEM (HRTEM) modelling was carried out using the Cerius2 code, according to a multislice methodology [9-10]. The module allows the customisation of the microscope

parameters being simulated. In this work, they were set to match the FEI CM200 device at Leeds (200 keV source voltage, C_s 1.2 mm), with thickness-defocus plots then being found. All (S)TEM results were simulated using Koch's QSTEM code [11], customised to use the following parameters throughout the simulations (based on those for SuperSTEM 1; 100 keV source voltage, −2.7 mm defocus, 0.005 mm spherical aberration (C_s), C_c 1.0 mm, 32 mrad convergence angle, dE 0.4 eV. The bright-field (BF) detector range was set as 0 – 4.3 mrad and for high-angle annular dark-field (HAADF) a range of 101 – 185 mrad was used.

3. Results and Discussion

The spiro-interstitial structure shown in Figure 1 was investigated. Initially, modelling was carried out using the full 289 atom structure found previously [6]. In order for these calculations to be tractable in terms of time and computational memory, a less dense *k*-point mesh was used than given in Table 1. EELS is a highly localised property, and the 289 atom structure can be 'cut-down' to the region of interest if a ground state calculation is utilised.

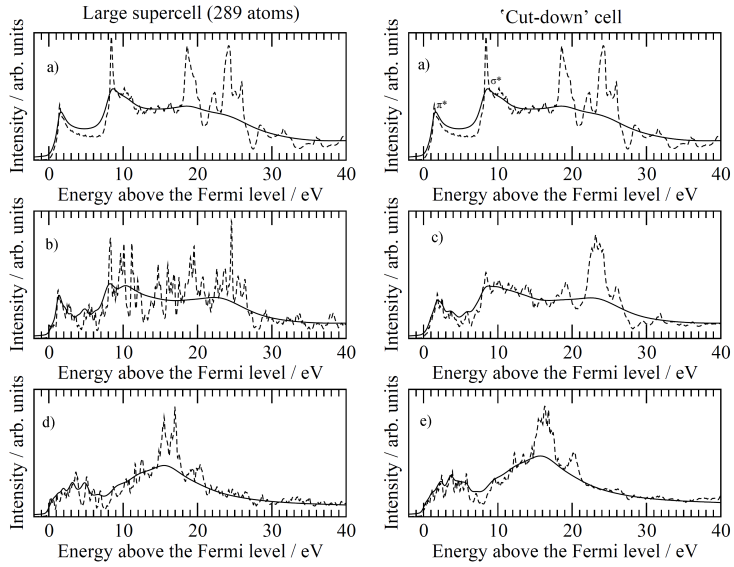

Figure 2. All plots shown are predicted carbon K edges. The dashed lines represent effectively unbroadened spectra, the solid lines show the spectra with the addition of energy-dependent final state lifetime broadening [14]. a) is shown twice. This plot is a bulk graphite carbon K edge prediction in the ground state. b) and c) Represent an edge in the spiro-interstitial model structures at a 'bulk-like' position remote from the interstitial, for the full 289 atom structure, and 'cut-down' structure respectively. d) and e) are the carbon K edge predictions for the spiro-interstitial position for the full 289 atom structure and 'cut-down' structure respectively.

For a position in either the large or 'cut-down' models that was remote from the spiro-interstitial, the prediction closely matches that of bulk. Therefore, changes we observe at the spiro-interstitial position itself can be considered valid. Comparing for example results a) and c) to e), there is broadening in the π^* region, suggesting strained sp^2 bonding, rather than all sp^2 character being eliminated. The relative intensity of the σ^* transition peak increases, and the energy position of the peak is shifted. These observations are arguably consistent with the spiro-interstitial structure, which is strained from ideal sp^3 bonding character as would be observed in spiro-pentane.

Bulk graphite was investigated. For a (100) projection, several phase reversals occur over typical TEM thicknesses or defocus ranges. For example, for a thickness of 49.2 nm, a phase reversal occurs approximately every 40 nm of sequential defocus change, approximately true of all thickness values that were investigated. For a given value of defocus, for example −50 nm, a phase reversal occurs approximately every 10 nm of thickness change. In terms of the spiro-interstitial, consider the results presented in Figure 3:

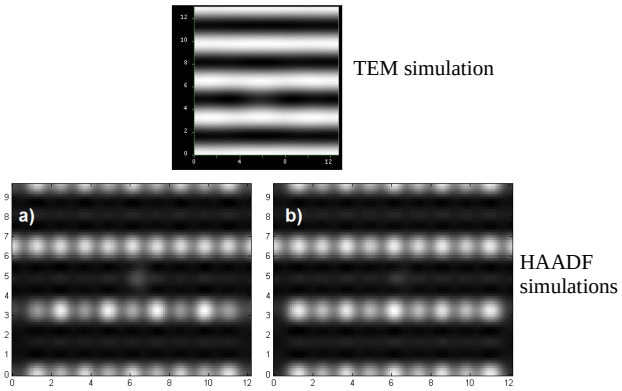

Figure 3. Various image simulations. The TEM simulation uses parameters as described in the methodology section for a CM200 device. The image is for zero defocus. In this case the spiro-interstitial was placed at the centre of a 14.67 Å thick 'sample'. a) and b) are both (S)TEM simulations carried out using QSTEM, according to parameters discussed in the methodology section of this proceeding. In a), the interstitial is at the edge of a 5.8 Å thick 'sample', and in b) it is at the centre of a 12.5 Å thick 'sample'.

4. Conclusions

Early-stage EELS modelling suggests that for a spiro-interstitial as compared to the bulk graphite carbon K edge, the π^* peak is broadened, and the σ^* peak shifted with an intensity increase relative to the π^*. These observations are consistent with the formation of a strained spiro-interstital. There is evidence for cross-linking defects in double-walled nanotubes (DWNT) that could reasonably be assumed to be due to spiro-interstitial formation or intimate Frenkel pairs [15], DWNT TEM imaging (side-on) having been achieved [16]. This simulation work further suggests that graphene-like ultrathin samples should be used if interstitials are to be observed in the TEM / (S)TEM.

References

[1] Zinkle S J, Busby J T 2009 *Mater. Today* **12** 12.
[2] Kelly B T, Brocklehurst J E 1971 *Carbon* **9** 783.
[3] Agranovich V M, Semenov L P 1964 *Journal of Nuclear Energy, Parts A/B Reactor Science Technology* **18** 141.
[4] Kelly B T. *Physics of Graphite*. Applied Science Publishers, London 1981.
[5] Heggie M I, Eggen B R, Ewels C P, Leary P, Ali S, Jungnickel G, Jones R and Briddon P R 1998 in *Fullerenes Vol. 6: Recent Advances in the Chemistry and Physics of Fullerenes and Related Materials (11th International Symposium),* eds. Kadish K M, Ruoff R S, Electrochemical Society: Pennington, N.J., 60-67.
[6] Latham C D, Heggie M I; Gámez J A; Suárez-Martínez I, Ewels C P and Briddon P R 2008 *J. Phys.: Condens. Matter* **20** 395220.
[7] Telling R H, Ewels C P, El-Barbary A A and Heggie M I 2003 *Nat. Mater.* **2** 333.
[8] Clark S J, Segall M D, Pickard C J, Hasnip P J, Probert M I J, Refson K and Payne M C 2005 *Zeitschrift für Kristallographie* **220** 567.
[9] Cowley J M, Moodie A F 1957 *Acta Cryst.* **10** 609.
[10] Saxton W O, O'Keefe M A, Cockayne D J H and Wilkens M 1983 *Ultramicros.* **12** 75.
[11] Koch C 2002 PhD Thesis, Arizona State University. *Determination of Core Structure Periodicity and Point Defect Density Along Dislocations.*
[12] Seabourne C R, Scott A J, Brydson R and Nicholls R J 2009 *Ultramicros.* **109** 1374.
[13] Seabourne C R, Scott A J, Vaughan G, Brydson R, Wang S G, Ward R C C, Wang C, Kohn A, Mendis B and Petford-Long A 2010 *Ultramicros.* **110** 1059.
[14] Moreau P, Boucher F, Goglio G, Foy D, Mauchamp V and Ouvrard G 2006 *Phys. Rev. B* **73**, 195111.
[15] Ewels C P, Telling R H, El-Barbary A, Heggie M I and Briddon P R 2003 *Phys. Rev. Lett*. **91** 025505.
[16] Urita K, Suenaga K, Sugai T, Shinohara H and Iijima S 2005 *Phys. Rev. Lett.* **94** 155502.

Acknowledgements

EP/I002588/1, EP/I003312/1 and related grants. CRS thanks the HPC team at the University of Leeds.